

Microscopic Color Measurements of Halftone Prints

Daniel Nyström

Linköping University, Dept of Science and Technology (ITN)
SE-60174 Norrköping, Sweden

Abstract

Modeling halftone print reproduction is difficult, mainly because of light scattering, causing optical dot gain. Most available models are based on macroscopic color measurements, integrating the reflectance over an area that is large relative the halftone dot size. The reflectance values for the full tone and the unprinted paper are used as input, and these values are assumed to be constant. An experimental imaging system, combining the accuracy of color measurement instruments with a high spatial resolution, allows us to measure the individual halftone dots, as well as the paper between them. Microscopic color measurements reveal that the micro-reflectance of the printed dots and the paper is not constant, but varies with the dot area fraction. By incorporating the varying reflectance of the ink and paper in an expanded Murray-Davies model, the resulting prediction errors are smaller than for the Yule-Nielsen model. However, unlike Yule-Nielsen, the expanded Murray-Davies model preserves the linear additivity of reflectance, thus providing a better physical description of optical dot gain. The microscopic color measurements further show that the color shift of the ink and paper depends on the halftone geometry and the print resolution. In this study, we measure and characterize the varying micro-reflectance of ink and paper with respect to properties of the halftones, using AM and FM prints of various print resolutions.

Introduction

Over the years, many models predicting the outcome of halftone prints have been proposed. The task is difficult, partly because of light scattering within the paper bulk, causing optical dot gain. Furthermore, the optical dot gain often co-exists with physical dot gain, caused by physical dot extension in the printing process. Understanding the physical nature of physical and optical dot gain in halftone prints is essential for accounting for the effect in order to improve print quality.

In the 1930s Murray and Davies published the first model to predict the output reflectance of a halftone print [1]. The mean reflectance R , is simply given by linear interpolation of the reflectance of the unprinted paper, R_p , and the full tone, R_i , weighted by the dot area fraction, a , as:

$$R(a) = aR_i + (1 - a)R_p \quad (1)$$

Since the reflected light from different areas is added to predict the overall reflectance, the Murray-Davies (MD) model preserves the linearity of photon additivity. It is, however, well known that the applicability of the model is very limited. The relationship of R versus a is in fact non-linear, due to light scattering in the paper substrate, causing optical dot gain.

In the 1950s, Yule and Nielsen proposed that the nonlinear relationship could be approximated by a power function [2]:

$$R(a) = \left(aR_i^{1/n} + (1 - a)R_p^{1/n} \right)^n \quad (2)$$

The Yule-Nielsen n -factor, accounting for light scattering in the paper, is an empirically derived constant, selected to provide the best fit to experimental data. However, the Yule-Nielsen (YN) model does not physically describe the phenomenon of optical dot gain, and the conservation of energy is lost when the nonlinear transform is applied to the reflectance values.

Notice that the fundamental assumption in these models is that the reflectance for the substrate and the ink is both uniform and constant. The inputs to the models are the reflectance values for the unprinted paper and for the full tone ink. It was, however, shown in the 1990s that the color of the halftone dots and the paper between them is not constant, but dependent on the dot area fraction [3]. The reflectance of the printed halftone dots, as well as the paper between them, decreases with increasing dot area coverage, due to light scattering in the substrate. An expanded Murray-Davies model was proposed, with the constants for paper and ink reflection replaced by the functions $R_i(a)$ and $R_p(a)$ [4]:

$$R(a) = aR_i(a) + (1 - a)R_p(a) \quad (3)$$

This model preserves the additivity of reflectance while the non-linear relationship between R and a caused by optical dot gain, is accounted for by using the functions $R_i(a)$ and $R_p(a)$. Naturally, the difficulty with this approach is to derive $R_i(a)$ and $R_p(a)$, i.e. the way that the reflectance of the ink and paper shift with the dot area. It is clear that it is not possible to measure these components using macroscopic color measurements, giving the averaged reflectance of the print.

Previous attempts to measure and characterize $R_i(a)$ and $R_p(a)$ have been made by point-wise measurements using a spectro-radiometer equipped with magnification lenses, as well as using histogram data from grayscale images of the prints [3-4]. However, the print resolutions of the prints used in these studies were low in comparison to the high-resolution prints of today.

In this work, we continue the approach of using microscopic color measurements to characterize and model halftone printing. An experimental image acquisition system, combining a high spatial resolution with colorimetric accuracy, allows us to measure the reflectance of the individual halftone dots, as well as the paper between them. In a preliminary study, we have shown that the expanded Murray-Davies model is applicable even for prints of considerably higher print resolutions [5]. We have also proposed an extension of the model to handle color prints, predicting CIEXYZ-values, by using 3D histograms in CIEXYZ color space. The focus of this study is to measure the micro-reflectance of the ink and paper, $R_i(a)$ and $R_p(a)$, for AM and FM prints of various

print resolution. The aim is to investigate how the varying micro-reflectance is related to halftone geometry and print resolution.

Experimental Setup

An experimental image acquisition system is used, specially designed for capturing microscopic images of prints and substrates. The images are captured using a monochrome CCD camera, with a resolution of 1360×1024 pixels and 12 bit dynamic range. It has previously been verified that the camera response is linear with respect to the intensity of the incident light [6]. The optics used is a macro system, allowing for various magnifications up to a maximal resolution corresponding to $1.2 \mu\text{m}/\text{pixel}$. The illumination is provided using a tungsten halogen lamp through optical fibers, which offers an adjustable angle of incidence. Color images are captured sequentially, using filters mounted in a filter wheel in front of the light source. Besides RGB-filters, the filter wheel also contains a set of 7 more narrow-band interference filters. The image acquisition system has previously been thoroughly calibrated and characterized, and models have been developed, allowing for colorimetric and multispectral image acquisition [6-7].

Grayscale images of the test prints in the study have been captured using the $45^\circ/0^\circ$ measurement geometry. The field of view was $2.7 \times 2 \text{ mm}$, giving a resolution corresponding to $2 \mu\text{m}/\text{pixel}$. All images are first corrected for dark current and CCD gain [6]. After calibration against a white reference, the pixel values in the grayscale images correspond to reflectance values.

The printed samples consisted of offset prints on coated paper, printed with amplitude modulated halftones (AM), as well as frequency modulated halftones (FM). The AM halftones used clustered dots and were generated for the screen frequencies 65, 100, 135 and 170 lpi. The FM halftones were generated for the print resolutions 150, 300, 600 and 1200 dpi, using an iterative method for optimal dot placement [8]. The nominal dot area coverage of the patches are 2, 5, 10, 15, ..., 90, 95, 98 and 100% respectively. The test charts were printed with a commercial 4-color offset press, and all the patches were printed using the same plate.

Macroscopic measurements of the spectral reflectance values of the printed color patches were derived using a Gretag Machbeth Spectrolino spectrophotometer, equipped with a UV filter, using the $45^\circ/0^\circ$ measurement geometry.

Methodology

Microscopic images, i.e. when the resolution of the images is high in relation to the resolution of the printed halftone, allow for measurements of the individual halftone dots, as well as the paper between them. To capture the typical characteristics of a large population of halftone dots, which may differ in their appearance, reflectance histograms are computed from the microscopic images.

A reflectance histogram is a plot of the frequency of occurrence of reflectance values in the images, as a function of the reflectance, R . For a perfectly reproduced halftone pattern, the histogram would be truly bimodal, with only two peaks corresponding to the reflectance of the ink and the paper. For a real print, however, the populations around R_i and R_p are typically spread out, due to the spread or blurring of the halftone dots, and to light scattering within the substrate.

From the reflectance histograms it is possible to measure the micro-reflectance of the ink, $R_i(a)$, and the paper, $R_p(a)$, by locating the peaks in the histogram. Figure 1 displays an example of a normalized histogram of reflectance values, for the full tone ($a=1$); the bare paper ($a=0$), and a 60% tint. It is clear from the positions of the peaks for the 60% tint that the reflectance values of the ink, $R_i(0.6)$, and paper, $R_p(0.6)$, have shifted with the dot area coverage, a .

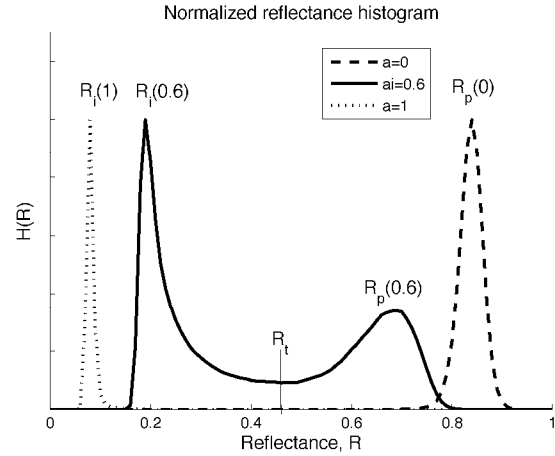


Figure 1. Normalized reflectance histogram for halftone prints of $a=0$, $a=0.6$ and $a=1$.

It is important that the dot area fraction, a , used in Eq. 3 corresponds to the physical dot area coverage, a_{phy} , which typically differs from the nominal dot area, a_0 , due to physical dot gain. The physical dot area fraction can be computed from the histogram, using a threshold value, R_t , as the limit between the ink and the paper, as:

$$a_{phy} = \frac{\int_0^{R_t} H(R) dR}{\int_0^1 H(R) dR} \quad (4)$$

A simple approach to define the threshold, R_t is to use the midpoint between the peaks corresponding to $R_i(a)$ and $R_p(a)$ in the histogram. When microscopic images of the prints are available, another possibility is to derive the threshold from the images. By using vertical and horizontal line scans across the halftone dots, R_t can be defined as the region of maximum rate of change in reflectance values, dR/dx [4]. An edge is a part of the image where the tone variation is large, and R_t , representing the boundary between the dot and the paper, is thus defined as the position having the steepest slope in reflection between dot and paper. To ensure that the threshold value is representative for all halftone dots, every tenth line in the image, both horizontally and vertically, are used when computing R_t . [5]

Experimental Results

Tables 1 lists the RMS errors between the measured mean reflectance and the predicted reflectance values, for all printed halftone patches. The expanded Murray-Davies model (Eq. 3) has

been used with $R_i(a)$ and $R_p(a)$ computed from grayscale histograms. The physical dot area coverage, a_{phy} , has been estimated using line scans from micro-scale images. Computations with the ordinary Murray-Davies (MD) model and the Yule-Nielsen (YN) model are also included for comparison. For Yule-Nielsen, the optimal n -value has been used, computed individually for each print. The best results are marked as bold in the table.

Table 1. RMS errors between measured and predicted mean reflectance values for AM and FM prints of various resolutions.

		MD	YN	n	Exp. MD
AM	65 lpi	0.0245	0.0071	1.38	0.0028
	100 lpi	0.0258	0.0073	1.45	0.0039
	135 lpi	0.0394	0.0074	1.99	0.0046
	170 lpi	0.0247	0.0052	1.62	0.0065
FM	150 dpi	0.0286	0.0094	1.39	0.0028
	300 dpi	0.0222	0.0051	1.34	0.0031
	600 dpi	0.0244	0.0051	1.45	0.0031
	1200 dpi	0.0216	0.0080	1.35	0.0030

As expected, the expanded Murray-Davies clearly outperforms the ordinary Murray-Davies. The results when employing the expanded Murray-Davies model are also generally better than the Yule-Nielsen model, using optimal n -factors. The estimated physical dot area, a_{phy} , has also been used for the MD and YN computations. Using the nominal dot area, a_0 , greatly increases the prediction errors for the MD-model and gives n -factors much larger than 2. Note that all Yule-Nielsen n -factors belong to the physically meaningful range, $1 \leq n \leq 2$, due to the use of the correct physical dot area, a_{phy} .

Figure 2 displays the measured reflectance values compared to the predicted reflectance using the model, as well as the reflection for the ink, $R_i(a)$, and for the paper, $R_p(a)$, estimated from the histograms for AM prints of various screen frequency. The corresponding values for the FM prints are given in Fig. 3.

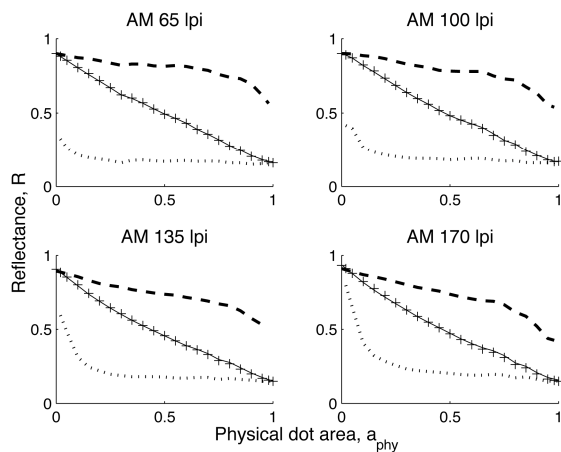


Figure 2. Measured mean reflectance (solid), predicted reflectance (+), $R_p(a)$ (dashed) and $R_i(a)$ (dotted). AM prints of various screen frequency.

It is clear from Figs. 2 and 3 that the micro-reflectance for the ink and the paper, $R_i(a)$ and $R_p(a)$, varies with the physical dot area coverage, a_{phy} . The variation of the reflectance of the paper, $R_p(a)$ is generally larger than that of the ink $R_i(a)$. The variation in reflectance values for both ink and paper increases with increasing screen frequency (AM prints) and print resolution (FM prints), and thus with decreasing dot size.

For the AM prints, the largest variations occur when a_{phy} approaches 0 and 1, i.e. when size of the dots and the paper between the dots become small. For the FM prints, the variation of the ink and paper reflectance is more linear with dot area coverage. This is because the effect of the light scattering is closely related to the dot size, giving $R_i(a)$ and $R_p(a)$ that is non-linear with respect to a for the AM prints, with varying dot size, and a more linear behavior for the FM prints, using constant dot size. The experimental findings in Figs. 2 and 3 demonstrate a close resemblance to simulations using point spread functions [9].

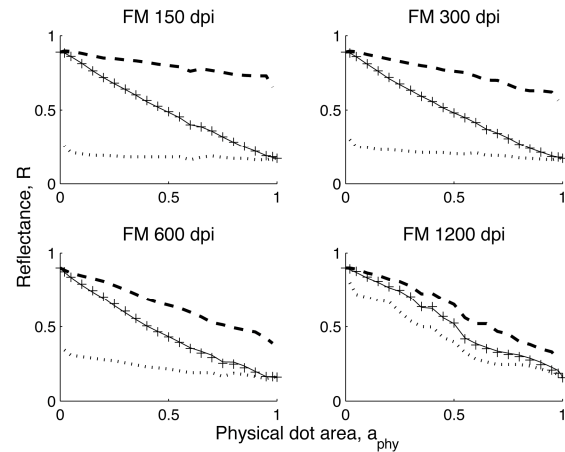


Figure 3. Measured mean reflectance (solid), predicted reflectance (+), $R_p(a)$ (dashed) and $R_i(a)$ (dotted). FM prints of various print resolutions.

Modeling $R_p(a)$ and $R_i(a)$

In a previous attempt to model the functions for the varying reflectance of the ink, $R_i(a)$, and paper, $R_p(a)$, the following functions have been proposed [4]:

$$R_i(a) = R_0(1 - (1 - t)a^w)(1 - (1 - t)a^v) \quad (5)$$

$$R_p(a_p) = R_0(1 - (1 - t)(1 - a_p^w))(1 - (1 - t)(1 - a_p^v)) \quad (6)$$

where R_0 is the bulk reflectance of the paper, t is the ink transmittance, a_p is the area coverage for the paper (i.e. $1 - a$), v is an empirical parameter said to be related to the softness of the dot edges, and w is an empirical parameter representing the effect of light scattering.

Figure 4 displays the results when the parameters w and v are derived using non-linear optimization software to provide the best fit to experimental data, minimizing the RMS error of the predicted and measured mean reflectance.

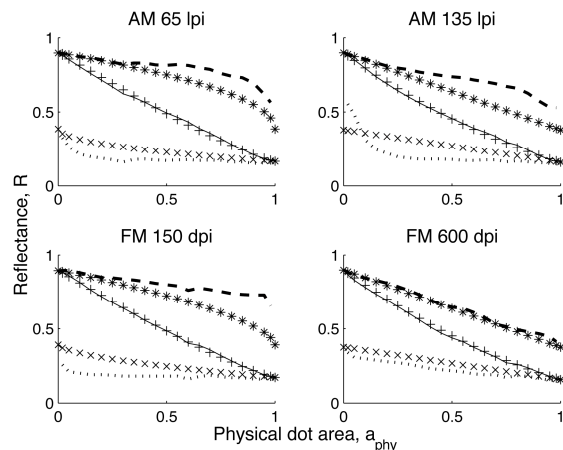


Figure 4. Mean reflectance: measured (solid) and predicted (+). $R_p(a)$: measured (dashed) and modeled (x). $R_i(a)$: measured (dotted) and modeled (*).

It is clear from Fig. 4, that even though the predicted mean reflectance fits the measured reflectance, producing small RMS errors, the modeled functions for $R_i(a)$ and $R_p(a)$, do not show a close resemblance to the experimental data. If w and v are instead optimized to fit the experimentally measured $R_i(a)$ and $R_p(a)$, the RMS error of the predicted mean reflectance increases dramatically. It is simply not possible to obtain a good fit to experimental data using the parameters w and v , equal for both $R_i(a)$ and $R_p(a)$, according to Eqs. 5 and 6. The functions, proposed after experiments on low-resolution digital prints, are clearly not general enough to deal with offset prints of higher resolutions.

Summary and Future Work

In this study we have used microscopic images to study how the reflectance of the printed dots and the paper between them vary with respect to the dot area fraction. The reflectance values of the ink, $R_i(a)$, and paper, $R_p(a)$, are estimated using histogram data, and the physical dot area fraction, a_{phy} , is estimated using line scans in the microscopic images. Alternative methods for estimating the physical dot area are described in Ref [10-11].

It was shown that the expanded Murray-Davies model, utilizing the varying reflectance $R_i(a)$ and $R_p(a)$, is valid even for prints of considerably higher print resolution than those used in previous studies. The prediction errors of the model were smaller than the results when employing the Yule-Nielsen model. However, unlike the YN model, the expanded MD model preserves the linear additivity of reflectance, thus providing a better physical description of halftone color reproduction.

The variation in reflectance values for the ink and paper, $R_i(a)$ and $R_p(a)$, increases with increasing print resolution, and thus with decreasing dot size. For the AM prints, the largest variations occur when a_{phy} approaches 0 and 1, i.e. when the area of the dots and the paper between the dots, respectively, becomes small. For the FM prints, using constant dot size, the variation of the ink and paper micro-reflectance is more linear with the dot area coverage. From these findings, it is obvious that the Murray-Davies and

Yule-Nielsen models, assuming constant reflectance of the ink and paper, must be fundamentally wrong.

A previously proposed model for $R_i(a)$ and $R_p(a)$, using the empirical parameters w and v , was applied to experimental data. When fitted against the mean reflectance, i.e. the macroscopic measurement, the model produces good predictions. However, when examining the modeled functions for $R_i(a)$ and $R_p(a)$ using microscopic measurements, it was not possible to obtain a good fit to experimental data.

Future work should be devoted to finding better models for $R_i(a)$ and $R_p(a)$, i.e. how the reflectance of the ink and the paper between the dots varies with dot area coverage. Especially, focus should be on relating these functions to properties of the printing process, such as the paper substrate, the printing method and the halftoning employed. Our previous extension of the model to handle color prints, predicting CIE XYZ values, was limited to single colorants only. In the future, the method should be further developed to handle the case of multiple, overlapping, colorants, i.e. into an expanded Neugebauer model, incorporating the varying reflectance of the different inks and the paper. Microscopic color measurements of halftone prints will provide a powerful tool in future research devoted to gain a deeper understanding of the complex process of halftone color reproduction.

References

- [1] A. Murray, Monochrome reproduction in photoengraving, J Franklin Institute, 221, 721 (1936).
- [2] J.A.C. Yule & W.J. Nielsen. The Penetration of Light Into Paper and Its Effect on Halftone Reproductions, Proc. TAGA, pg. 65. (1951).
- [3] P.G. Engeldrum, J. Imaging. Sci. and Technol., Vol.38, No. 6, pg 545 (1994).
- [4] J.S. Arney, P.G. Engeldrum, and H. Zeng, J. Imaging. Sci. and Technol., Vol.39, No. 6, pg 502 (1995).
- [5] D. Nyström, A Close-Up Investigation of Halftone Color Prints” Proc. TAGA, pg. 347. (2008).
- [6] D. Nyström, High Resolution Analysis of Halftone Prints – A Colorimetric and Multispectral Study, Dissertations No. 1229, Linköping University, (2008).
- [7] D. Nyström, Reconstructing Spectral and Colorimetric Data Using Trichromatic and Multi-channel Imaging, Proc. Ninth International Symposium on Multispectral Color Science and Application, pg 45. (2007).
- [8] S. Gooran, High Quality Frequency Modulated Halftoning, Dissertations No. 668, Linköping University, (2001).
- [9] L. Yang, R. Lenz, Reiner and B. Kruse, Light Scattering and Ink Penetration Effects on Tone Reproduction. J. Opt. Soc. Am. A, 18, pg 360, (2001).
- [10] D. Nyström & L. Yang, Physical and Optical Dot Gain: Separation and Relation to Print Resolution, Proc. Advances in Printing and Media Technology, Vol. 36, pg 337. (2009).
- [11] M. Nemedanian & S. Gooran, High Resolution Analysis of Optical and Physical Dot Gain, Proc. TAGA. (2010).

Author Biography

Daniel Nyström received his M.Sc. degree in Media Technology from Linköping University, Sweden, in 2002 and his Ph.D degree from the same university in 2009. He is currently working as a research associate in the Digital Media group at the Dept. of Science and Technology, Linköping University. His current research interests include color science, print quality, paper optics and image processing.